

Criticality and universality in a generalized earthquake model

C. J. Boulter and G. Miller

Department of Mathematics, School of Mathematical and Computer Sciences, Scott Russell Building, Heriot-Watt University, Edinburgh EH14 4AS, United Kingdom

(Received 4 June 2004; revised manuscript received 20 October 2004; published 13 January 2005)

We propose that an appropriate prototype for modeling self-organized criticality in dissipative systems is a generalized version of the two-variable cellular automata model introduced by Hergarten and Neugebauer [Phys. Rev. E **61**, 2382 (2000)]. We show that the model predicts exponents for the event size distribution which are consistent with physically observed results for dissipative phenomena such as earthquakes. In addition we provide evidence that the model is critical based on both scaling analyses and direct observation of the distribution and behavior of the two variables in the interior of the lattice. We further argue that for reasonably large lattices the results are universal for all dissipative choices of the model parameters.

DOI: 10.1103/PhysRevE.71.016119

PACS number(s): 05.65.+b, 91.30.Px, 45.70.Ht, 64.60.Ak

I. INTRODUCTION

For more than a decade the application of self-organizing cellular automata models to the study of earthquake and landslide dynamics has generated considerable controversy. The concept of self-organized criticality (SOC) was first introduced by Bak, Tang, and Wiesenfeld (BTW) [1,2] in the context of a simple sandpile model which is driven by the random addition of sand grains and relaxes via a sequence of avalanches. The model evolves to a critical state where characteristic scales are lost and the avalanche distribution displays power law behavior. In the BTW model the number of grains of sand is conserved except at the boundaries of the system, and it has been shown that this conservation law is crucial for criticality in the model [3].

In contrast phenomena such as earthquakes and landslides which experimentally display scale-invariant event distributions over many decades are dissipative. In both of these cases the probability density for events of “energy” E is of the form $P(E) \sim E^{-\tau}$ where the exponent is in the range $\tau \approx 1.8-2.1$. Unsurprisingly these exponents are not recovered by the conservative BTW model. As a result a variety of dissipative models have been introduced in order to better capture the underlying behavior, with the most successful being the Olami-Feder-Christensen (OFC) earthquake model [4]. In the OFC model each node (i, j) on a square lattice is associated with a continuous-state variable or energy u_{ij} . Initially the energies are assigned random values in the interval $[0, 1)$. The system is then slowly driven in such a way that the energy at all the sites increases uniformly until one of the sites reaches the threshold $u_{ij} = 1$ and is termed supercritical. When this happens an avalanche occurs at a time scale much quicker than the driving speed. The supercritical site relaxes, with its energy being distributed to four neighbors, u_{neigh} , according to

$$u_{\text{neigh}} \rightarrow u_{\text{neigh}} + \alpha u_{ij}, \quad u_{ij} \rightarrow 0. \quad (1.1)$$

If any of the neighboring sites become supercritical (i.e., $u_{\text{neigh}} \geq 1$) as a result of this process, they also topple according to the same rules. The avalanche continues until all node values are below the threshold, at which stage the driving

process proceeds until the next event is triggered. The parameter α measures the level of dissipation in the toppling process. If $\alpha = 0.25$, the energy is conserved, while for $\alpha < 0.25$ the system is clearly nonconservative. The question of whether the OFC model is truly critical in this case has attracted a great deal of attention in recent years. In the random-neighbor (RN) version of the model it has been analytically established that the system is never critical in the nonconservative regime [5,6]. In the nearest-neighbor (NN) version there is an increasing body of numerical evidence again suggesting that the model is only critical in the conservative limit [7–12]. Furthermore, for values of α at or close to the conservative limit one finds a density function exponent significantly smaller than that observed in nature, with $\tau \approx 1.2$ for $\alpha = 0.25$ and $\tau \approx 1.6$ for $\alpha = 0.24$. For smaller values of α there is clear numerical evidence that the model is not critical [9,11]; however, one can fit an exponent in the range $\tau \in [1.8, 2.1]$ across several decades of event sizes, providing encouragement that the nonconservative OFC model captures some important features of real dissipative systems [12,13].

In this paper we extend a two-variable lattice cellular automaton model recently introduced by Hergarten and Neugebauer (HN) [14]. In Sec. II we define the model and, via a preliminary investigation of event size distributions, argue that the model may well be both critical and have a density function exponent that is in agreement with physically observed distributions. Via analysis and simulation we study the random-neighbor version of the two-variable model in Sec. III, and on the basis of this study we conclusively demonstrate that the random-neighbor model is only critical in the limit when the variables are conserved. In contrast, in Sec. IV we analyze the nearest-neighbor version of the model and show that an extensive inner region of the system is critical for all choices of conservation level. Our main results and conclusions are summarized in Sec. V.

II. DEFINITIONS AND PRELIMINARY RESULTS

The motivation behind the OFC model is to identify the key elements that lead to the apparent ubiquity of SOC in

nature. In this sense one wants to find the simplest “toy” model which captures this behavior. However, as discussed above the OFC model is not sufficient in this respect and hence we look for an alternate model which is both critical *and* dissipative. A promising candidate has recently been proposed by Hergarten and Neugebauer [14,15], initially in the context of modeling landslides. In the BTW and OFC models an avalanche begins when the variable in the model reaches a threshold value, which can essentially be understood as being when the local slope or gradient of the surface is sufficiently large. To allow for other elements in their model HN have incorporated two variables u_{ij} and w_{ij} associated with each site in the lattice. Here we propose a generalization of the HN two-variable model and provide evidence that, unlike the OFC model, it is genuinely critical.

The original HN model is physically motivated by appealing to the ideas of toppling in avalanches or landslides for which one imagines many factors or variables might be relevant [15]. Avalanches are more likely to start where the local height differences are large; hence, the dominant factor is probably related to geometry. Physically the corresponding toppling process is approximately conservative associated with the movement of particles from one site to its neighbors. In addition there are nongeometric factors which also play a role in determining when and where an avalanche starts. For example, it is known that regardless of surface geometry the chance of a landslide increases over time due to a slow weakening of the failure plane, such features change nonconservatively during a landslide. In our model based on a square lattice we assume the conserved variables (local slopes or mass) are represented by u_{ij} , while the nonconserved elements are contained in w_{ij} . The two variables are initially distributed with random values drawn from a uniform distribution between 0 and 1. The product of the two variables determines the likelihood of an avalanche starting at a particular site and is used to measure the local “energy” or stress. If the energy $u_{ij}w_{ij} < 1$ at all sites, the system is stable and we assume that both variables are slowly, but uniformly, driven across the entire lattice (for simplicity we assume the variables are driven at the same rate; however, the results that follow are recovered for any choice of driving rates). This continues until at some site the energy, which increases nonlinearly in this model, reaches the threshold $u_{ij}w_{ij} = 1$ at which point an avalanche is initiated. The supercritical site relaxes according to

$$u_{\text{neigh}} \rightarrow u_{\text{neigh}} + \frac{1}{4}u_{ij}, \quad u_{ij} \rightarrow 0, \quad w_{ij} \rightarrow \epsilon w_{ij}. \quad (2.1)$$

For the nearest-neighbor version of the model the adjacent sites on the lattice are the appropriate neighbors. Later we also consider a random-neighbor two variable model in which for each toppling site the u_{neigh} are selected at random from the lattice. The variable w is not redistributed during the topple, and the parameter ϵ , which is assumed to be in the range $0 \leq \epsilon \leq 1$, measures the level of dissipation. If $\epsilon = 1$, both u and w are conserved during the topple; conversely, if $\epsilon < 1$, the toppling rule is dissipative in the variable w . As in the OFC model, if any neighboring sites become supercritical (i.e., $u_{\text{neigh}} \geq 1$), the avalanche continues using the same toppling rule until a stable state is reached.

Open boundary conditions are employed at the edges of the lattice providing the only form of dissipation in the $\epsilon = 1$ limit.

The HN model discussed above is recovered by choosing $\epsilon = 0$ [14]; in this limit, no site can ever topple more than once during a single avalanche. Hergarten and Neugebauer found that the nearest-neighbor version of their model produced an event size distribution with slope exponent of approximately 2 consistent with observations. For the generalized model we also start by considering the more physically relevant nearest-neighbor model. We have analyzed the probability distribution $P_L(s; \epsilon)$ of events of size s in a system of linear size L (i.e., a lattice of size $L \times L$) for fixed ϵ . For all values of ϵ simulated log-log plots of $P_L(s; \epsilon)$ versus s reveal approximately straight lines, suggesting possible SOC. Furthermore, the corresponding slope exponents satisfy $\tau = 1.90 \pm 0.10$ for all $\epsilon \leq 0.9$. The precise behavior for $0.9 < \epsilon < 1$ is difficult to elucidate from simulations due to increasing finite-size effects coupled with increased average avalanche sizes yielding a large transient period in the system (see also Sec. IV). As a result we can only crudely approximate the asymptotic slope exponent resulting in $\tau = 1.90 \pm 0.20$ in this range. Thus for all $\epsilon < 1$ we predict a slope exponent fully consistent with observations in nature.

Comparing results for different lattice sizes suggests that finite-size effects are important and are particularly noticeable for larger choices of ϵ . These effects lead to a deviation from linearity in log-log plots of $P_L(s; \epsilon)$ for small L . This behavior can be further investigated by using a finite-size scaling (FSS) hypothesis to try and collapse the data for fixed ϵ . The FSS ansatz states that

$$P_L(s; \epsilon) \sim L^{-\beta} F_\epsilon(s/L^D), \quad (2.2)$$

where F_ϵ is an appropriate scaling function and β and D are exponents that describe the scaling of the distribution function. The slope exponent is related to these exponents according to $\tau = \beta/D$. FSS plots for $\epsilon = 0, 0.2$, and 0.8 are shown in Fig. 1(a) using $\beta = 3.84$ and $D = 2$ corresponding to $\tau = 1.92$ (in this figure the data have been binned for improved resolution).

In general there is excellent data collapse for the larger system sizes considered, with deviations for small L . To more carefully examine the behavior of the tails of the probability distributions it is instructive to plot $s^\tau P_L(s; \epsilon)$ versus s/L^D which is similar to multiscaling the data [12,13,16]. Our results are shown in Fig. 1(b). For the two smaller choices of ϵ the data collapse is still good even on this exaggerated scale. For $\epsilon = 0.8$ the finite-size effects are much stronger, suggesting that if FSS is appropriate, it will only collapse the data for systems somewhat larger than $L = 600$.

A further interesting feature of the data is strong evidence of universality for all dissipative choices of ϵ . In particular, for fixed L one finds that the distributions $P_L(s; \epsilon)$ overlay one another for a range of ϵ values (excluding the cutoff region where $s \sim L^2$). More specifically for a particular choice of the dissipation parameter— $\epsilon = \epsilon_0 < 1$, say—one can find a crossover system size $L_\epsilon(\epsilon_0)$ such that for $L \geq L_\epsilon(\epsilon_0)$ there is a universal distribution $P_L(s; \epsilon)$ for $0 \leq \epsilon \leq \epsilon_0$. Due to

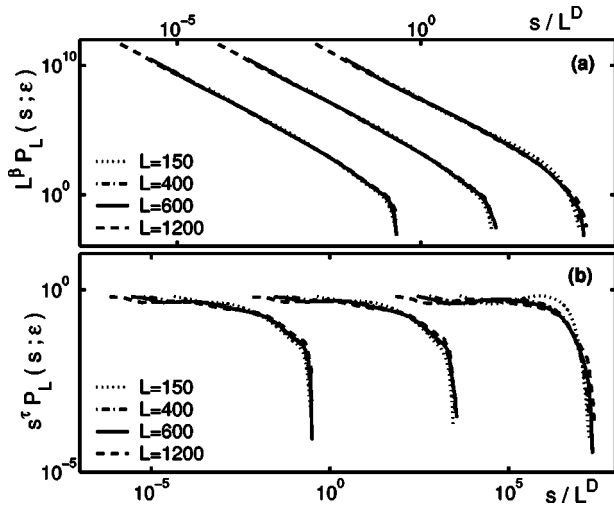


FIG. 1. Scaling plots of $P_L(s; \epsilon)$ for the two-variable model with $\epsilon=0, 0.2$, and 0.8 . Exponents $\beta=3.84$ and $D=2$ have been used corresponding to a slope exponent of $\tau=1.92$. Standard finite-size scaling has been used in (a) where for clarity the $\epsilon=0.2$ and 0.8 curves have been shifted right by two and four decades, respectively. In pane (b) the modified finite-size scaling plots discussed in the main text are shown. In this case the $\epsilon=0.2$ and 0.8 curves have been shifted right by four and eight decades respectively.

the finite-size effects discussed above, one finds that the crossover value $L_\epsilon(\epsilon_0)$ increases as ϵ_0 increases, with, for example, $L_\epsilon(0.2) \approx 300$ and $L_\epsilon(0.4) \approx 600$. As a result we believe the original HN model (where $\epsilon=0$) should capture all of the important features of the dissipative systems, while being the most efficient to study via simulation. In the conservative limit one recovers the $\alpha=0.25$ OFC result with a slope exponent $\tau \approx 1.2$. Thus it appears the conservative choice $\epsilon=1$ is in some sense a singular limit of the model. For arbitrarily large systems one would observe universal behavior for all dissipative choices of ϵ with distinct behavior in the conservative limit.

In summary, on the basis of preliminary studies we have shown that there is good evidence of power-law type behavior for all choices of the conservation parameter ϵ . The resulting slope exponent is consistent with observed phenomena in the nonconservative cases, and there is some evidence of finite-size scaling consistent with criticality. In the next two sections we examine the random- and nearest-neighbor models in more detail to further clarify their behavior.

III. RANDOM-NEIGHBOR TWO-VARIABLE MODEL

In this section we study the random-neighbor version of the two-variable model, which can be viewed as a mean-field approximation to the nearest-neighbor model. This allows us to determine the importance of spatial correlations for the model and has the benefit of being easier to analyze.

As mentioned above we know one of the features that a model must exhibit to be considered as having SOC characteristics is a power law in the probability distribution function. Hence we start by analyzing log-log plots of the probability distributions of avalanche sizes for various ϵ values

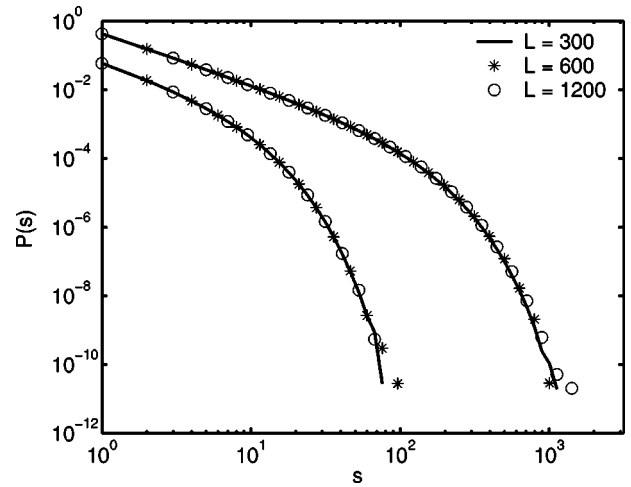


FIG. 2. Probability distributions of avalanche sizes in the random-neighbor two-variable model for $\epsilon=0$ (lower curve) and $\epsilon=0.8$ (upper curve). For clarity the lower curve has been shifted down one decade.

and system sizes. For small ϵ there is no clear region of power-law-type behavior, but as ϵ is increased there is more evidence for a straight line fit. Finally as $\epsilon \rightarrow 1$ there is a definite power law with slope exponent $\tau \rightarrow 1.5$, identical to the exponent found for the conservative RN OFC model [17]. In Fig. 2 the probability distributions for $\epsilon=0$ and $\epsilon=0.8$ are shown for a range of system sizes $L=300, 600$, and 1200 . The results for $\epsilon=0$ are shifted for clarity and in all cases the data have been binned in order to see the overlay of the different system sizes. From the results shown in Fig. 2 we see that a power law could not be fitted to the results for $\epsilon=0$ but when $\epsilon=0.8$ there is a region where a straight line could be fitted before the exponential tail, suggesting that for small ϵ the model is not critical. Furthermore, the plot shows that for a fixed ϵ and various L , the probability distributions overlay one another. Hence the model lacks scale invariance since the largest event size is not growing with L , and therefore could not be classed as displaying SOC behavior. Similar results are found for all choices of $\epsilon < 1$ studied.

To understand the model better we investigate the distributions of the energy variables u and ω . For all $\epsilon < 1$ we find that the distribution for the variable ω covers only a small range with all values closely bunched. Looking at Fig. 3 where we have plotted the distribution of the u variable for a selection of ϵ values, it is clear that as ϵ is increased towards 1 the distributions become more peaked with the locations of the peaks moving to the right. When $\epsilon=1$ the peaks are at $u/u_m \approx 0, 0.31, 0.62$, and 0.93 where u_m is the maximum u value measured across the system. Comparing this result with the RN OFC model when $\alpha=0.25$, shown as the lowest curve in Fig. 3, reveals that the distributions are very similar. This suggests that any theoretical results developed for the conservative RN OFC model may also fit the conservative RN two-variable model, indeed we believe that our model essentially reduces to the conservative OFC model in the limit $\epsilon \rightarrow 1$ (albeit with different threshold values at each site). Thus we believe the model is critical in this limit.

Further evidence that the random-neighbor model is only critical in the $\epsilon=1$ limit can be found by examining the

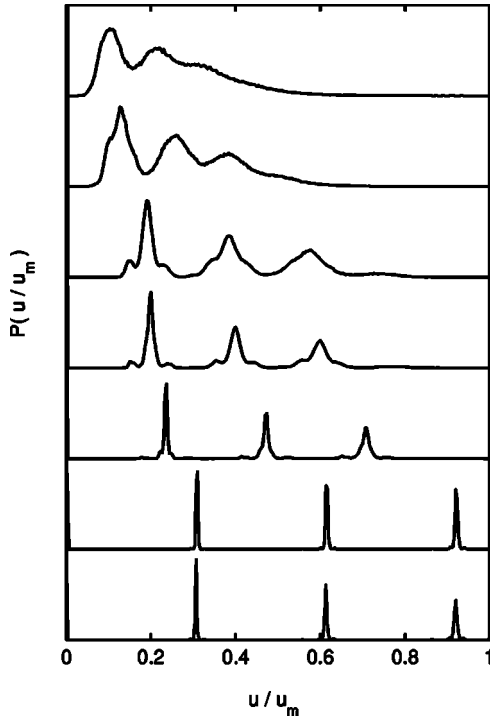


FIG. 3. Probability distributions of energy values u/u_m from simulations with $L=600$. From top to bottom the curves correspond to $\epsilon=0, 0.4, 0.8, 0.9, 0.95$, and 1 . The bottom curve corresponds to the RN OFC model when $\alpha=0.25$.

branching rate σ . Hence we numerically simulate the model to calculate σ for various ϵ and system sizes L . The branching rate is defined as the average number of supercritical descendants generated when each supercritical ancestor topples [17]. In the simulations we calculate σ in two slightly different ways. First we allow each toppling site to topple to either two, three, or four neighbors with the appropriate probabilities for modeling a system having a boundary (edges and corners); this is necessary to provide dissipation in the conservative limit $\epsilon=1$.¹ From these results we linearly extrapolate to estimate σ for an infinite-size system. In the second method we assume that each site has precisely four neighbors, naively modeling an infinitely large system. In Table I we provide our results for the two different methods.

For small ϵ the extrapolated results from the first method and the results for the second method are in excellent agreement. As ϵ increases ($\epsilon > 0.9$) there is a slight discrepancy; we believe that larger systems are required in order to be able to more accurately extrapolate because the average avalanche size is becoming large, leading to noticeable finite-size effects. The results confirm that the model is only critical in the conservative case.

IV. NEAREST-NEIGHBOR TWO-VARIABLE MODEL

For the remainder of this paper we concentrate on the nearest-neighbor two-variable model for which we found en-

¹In particular we assign two neighbors with probability $4/L^2$ and three neighbors with probability $4(L-2)/L^2$ reflecting the number of corner and edge sites, respectively, on a square $L \times L$ lattice. In all other cases four neighbors are assigned.

couraging preliminary results in Sec. II. Our study is based on extensive simulations of the model for a variety of system sizes L and conservation parameter levels ϵ . In order to enable large scale simulations we have employed a linked-list data structure similar to that introduced by Grassberger for the OFC model [7]. The only significant difference compared to the OFC model is that, due to the nonlinear form of the update rule for the two variable model, it is not those sites with uw closest to the threshold (i.e., the smallest $1-uw$) but rather those with the smallest $[-(u+w) + \sqrt{(u-w)^2 + 4}]/2$ which will seed the next avalanche. Using this algorithm reduces CPU time by typically three orders of magnitude compared with a naive implementation of the model rules.

In our simulations random initial data in the range $[0,1)$ is chosen for both u and w , and the model is run according to the rules given in Sec. II. One expects a transient period during which the system organizes towards a stationary state; it is important to wait until after this transient phase before collecting data. We find that the usual indicator of transient behavior, the average avalanche size, rapidly converges but that the distributions of the u and w variables continue to organize over a much longer period. Thus we believe that monitoring the maximum u value across the lattice gives the best guide to when the transient phase is passed, with this value approaching a constant level $u_{\max}(L, \epsilon)$ for each choice of L and ϵ . We further find that for a given choice of ϵ the approach to the maximum u value follows a simple scaling pattern for most choices of L . In particular, if $u^+(n_s; L, \epsilon)$ is the maximum value of u after n_s avalanches, then we find data collapse by plotting $u^+(n_s; L, \epsilon)/L$ versus $n_s/L^{\gamma(\epsilon)}$ for an appropriate choice of exponent $\gamma(\epsilon)$. Consequently the number of avalanches that need to be simulated to reach the stationary state grows like L^γ . For example the results for $\epsilon=0$ with $\gamma=3.74$ are shown in Fig. 4.

The only exception to this scaling found occurs for sufficiently small systems $L < L_c$ say, where L_c increases from $L_c \approx 50$ for $\epsilon=0$ to $L_c \approx 600$ for $\epsilon=0.95$. For $\epsilon < 0.9$ the exponent γ varies slowly with $\gamma(\epsilon) \approx 3.74 + \epsilon/10$, while γ grows more rapidly as $\epsilon \rightarrow 1$. We further find that the limiting value $u_{\max}(L, \epsilon)$ satisfies

$$u_{\max}(L, \epsilon)/L = \lim_{n_s \rightarrow \infty} u^+(n_s; L, \epsilon)/L \approx 0.554\sqrt{1-\epsilon} \quad (4.1)$$

for all ϵ . The maximum u value vanishes as $\epsilon \rightarrow 1$ as is to be expected since in this limit the w values at all sites grow during the driving phase and remain fixed during the toppling phase of the avalanche. Thus one must find that the corresponding u values in the stable state decrease towards zero as the number of avalanches increases.

A. Distributions of u and w

The log-log plots of the probability distributions $P_L(s; \epsilon)$ shown in Sec. II give encouragement that the nearest-neighbor two-variable model may genuinely display self-organized criticality. Further evidence for criticality can be found from explicit examination of the distributions of the variables u and w in the interior of the lattice. To begin we examine $P_u(u)$, the probability distribution for the u variable.

TABLE I. Branching rate σ for the RN two-variable model calculated from simulations for a range of ϵ and L values. Columns 2–5 show results and extrapolations ($L \rightarrow \infty$) when two, three, or four neighbors are chosen at random (see main text). Columns 6 and 7 show the corresponding results when four neighbors are always chosen.

ϵ	Two, three, or four random neighbors				Four random neighbors	
	$L=300$	$L=600$	$L=1200$	$L \rightarrow \infty$	$L=300$	$L=600$
0.0	0.5159 ₁	0.5169 ₁	0.5173 ₁	0.5179 ₃	0.5178 ₁	0.5178 ₁
0.2	0.5733 ₁	0.5743 ₁	0.5749 ₁	0.5754 ₃	0.5754 ₁	0.5754 ₁
0.4	0.6443 ₁	0.6455 ₁	0.6461 ₁	0.6467 ₃	0.6466 ₁	0.6466 ₁
0.6	0.7336 ₁	0.7349 ₁	0.7356 ₁	0.7364 ₃	0.7362 ₁	0.7362 ₁
0.8	0.8516 ₁	0.8532 ₁	0.8539 ₁	0.8547 ₃	0.8547 ₁	0.8547 ₁
0.95	0.9778 ₁	0.9792 ₁	0.9798 ₁	0.9806 ₆	0.9801 ₁	0.9801 ₂
1.00	0.99975 ₂	0.99995 ₂		1.0000 ₃		

We have seen above that for each choice of L and ϵ there is a maximum value $u_{\max}(L, \epsilon)$ that the variable u takes. In Fig. 5 we plot the (appropriately normalized) distribution P_u against $u/u_{\max}(L, \epsilon)$ for $L=600$ and a range of ϵ values.

We note that the distributions overlay one another regardless of the choice of ϵ ; an equally convincing overlay is found if we also vary the system size. We further observe that the distribution has significant peaks at $u/u_{\max} = 0, \frac{1}{4}, \frac{1}{2}$, and $\frac{3}{4}$. These become more emphatic if we look at the distribution of u values over an interior sublattice of size $N \times N$ at the center of the full system. The results for a range of N are shown in Fig. 6.

From this we can see that the system organizes in such a way that near the center of the lattice all sites take a u value which is approximately an integer multiple of $u_{\max}/4$. This is clearly demonstrated in Fig. 7 which shows a snapshot of the u values in the middle 60×60 portion of the $L=1200, \epsilon=0.2$ system.

We discuss these findings further at the end of this subsection once we have established the corresponding distribution of the w variable.

We saw in Fig. 5 that the $P_u(u)$ distribution was essentially the same for any choice of L and ϵ . Connected to this is the observation that the distribution is stationary in the

sense that if we take a snapshot from any stable distribution we find the same results. The situation is more complicated for the corresponding w distribution $P_w(w)$. In this case we find that the overall shape remains approximately the same from one snapshot to another but the distribution does display significant movement. Concentrating on the interior of the system we observe that almost all sites take one of a handful of w values. The locations of the peaks move for later snapshots because w is increased during the driving phase between avalanches [we explain why this driving is significant for $P_w(w)$ but not $P_u(u)$ below]. For each ϵ we find peaks in the distribution only in the range $\epsilon \leq w/w_m \leq 1$ where w_m is the maximum value of w observed in the box over a large number of stable distributions. Watching movies of the distributions develop over time reveals that peaks move to the right until they reach $w=w_m$ when the corresponding sites topple and so the peak is reassigned to $w=\epsilon w_m$. This suggests that all sites in the box with a matching w value topple as part of a single avalanche. In Fig. 8 we show a snapshot of the w values in the middle 300×300 portion of the $L=1200, \epsilon=0.2$ system.

This shows that large connected patches of the system take the same w value. Within patches there are sometimes smaller patches of sites which all take another single w value. Each patch corresponds to a peak in $P_w(w)$ with a

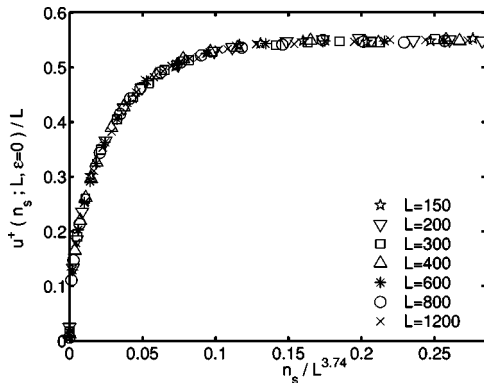


FIG. 4. Scaling plot of the growth of the maximum u value across the lattice (u^+) as the number of avalanches (n_s) grows. The results shown are for the case $\epsilon=0$ and a variety of lattice sizes as indicated.

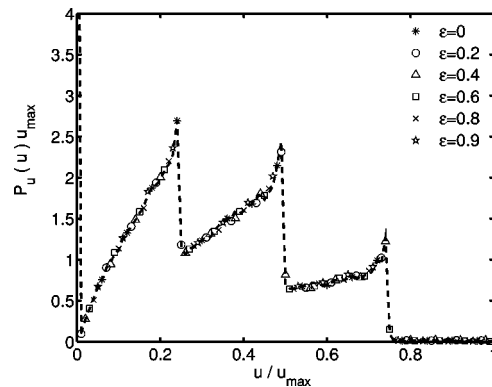


FIG. 5. The scaled probability distribution of the u variable across the lattice with $L=600$ and a range of ϵ values as indicated. The dotted line shows the complete set of data for the $\epsilon=0$ case.

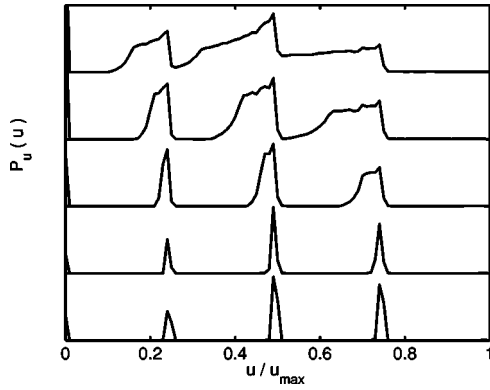


FIG. 6. The probability distribution of the u variable across interior $N \times N$ lattices with (from top to bottom) $N=4L/5$, $3L/5$, $2L/5$, $L/5$, and $L/10$.

height proportional to the size of the patch. The results described above indicate that when one site in a patch topples, nearly all other sites in the patch topple in the same avalanche.

Combining our results for $P_u(u)$ and $P_w(w)$ near the center of the lattice leads to a simple picture for the dynamics of the two-variable model. If we consider a box of size $N \times N$ at the center of the lattice, one finds patches of fixed w values of scales up to the box size and u values approximately at integer multiples of $u_{\max}/4$. The system is driven until $uw = 1$ at some site when an avalanche starts. According to Eq. (4.1) u_{\max} is large for large L and hence there is no noticeable change in $P_u(u)$ during the driving phase whereas there is a visible change in $P_w(w)$ because the maximum w value in a box near the center of the lattice, w_m , is small with $w_m \approx 1/u_{\max}$. Within the patch of the seed site all sites topple in the avalanche in an analogous manner to a large avalanche in the BTW sandpile model. It is possible that neighboring patches also topple within the avalanche if there had previously been no site with $u \approx u_{\max}$ even though $wu_{\max} \geq 1$ for the w value in that patch. Since all w values in a patch are reassigned in the same avalanche, they remain as a single

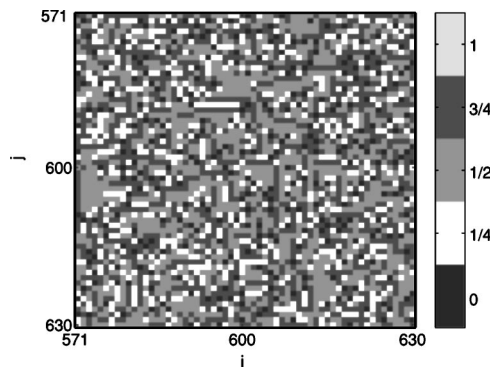


FIG. 7. A snapshot of the u values in the center 60×60 box for the case of an $L=1200$, $\epsilon=0.2$ system. Here i and j represent the coordinates of the sites in the lattice. All sites in this sublattice take a value of $u/u_{\max}=0, 0.25, 0.50, 0.75 \pm 0.0023$ and are shaded as shown in the color bar. In this snapshot there is no site with $u \approx u_{\max}$.

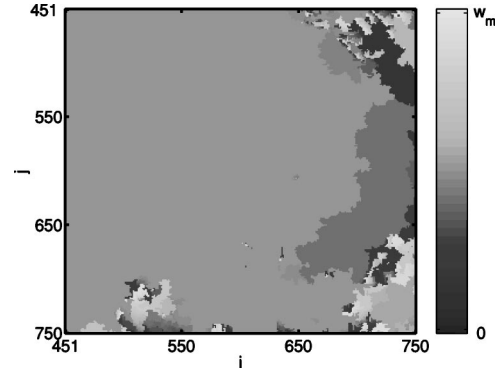


FIG. 8. A snapshot of the w values in the center 300×300 box for the case of an $L=1200$, $\epsilon=0.2$ system. The values (between 0 and w_m) are shaded as shown in the color bar, and i and j represent the coordinates of the sites in the lattice.

patch after the avalanche has occurred. We show below that a simple periodically repeating pattern of avalanches is prevented, however, by the outer layers which do not fit with this scheme.

B. Quantitative formalism for criticality

The large patches of constant w values near the center of our lattices observed in Sec. IV A are somewhat reminiscent of the distributions of spins in an Ising or multistate Potts model at the critical temperature. In this subsection we aim to capitalize on this similarity in order to develop another formalism for identifying criticality. We require several features for critical behavior: First, the dimension of the largest patch of fixed w (which we may identify as a “correlation length”) should diverge in the infinite size limit. Second, we need to confirm that when an avalanche starts in a patch, all sites in that patch topple in the same avalanche (in the limit of $L \rightarrow \infty$). Finally, we require patches on all scales up to the lattice size. We examine these requirements below leading to an improved understanding of the system dynamics and further evidence that the model is genuinely critical.

Initially we devise a quantity to measure the likelihood that all sites within a particular w patch topple in the same avalanche. We know that the distribution of variables is more organized near the center of the lattice, so we choose a measure which can be defined layer by layer (where layer 1 contains all sites on the boundary of the lattice and layer $L/2$ contains the innermost four sites). At the start of each avalanche we measure the w value of the seed site, w_s . Then for each layer i we count the number of sites with $w=w_s$ which receive a contribution from a toppling neighbor during the avalanche— n_i^{rec} , say (a site is only counted once in any single avalanche). We further count n_i^{top} , the number of sites in layer i that topple and had $w=w_s$, specifically excluding the seed site. We repeat this process over many avalanches and define the *layer patch branching rate* via

$$p_{\sigma}^{(i)} = \sum n_i^{\text{top}} / \sum n_i^{\text{rec}}, \quad (4.2)$$

where the sums are taken over all avalanches. Our results for the most dissipative choice $\epsilon=0$ and a range of system sizes are shown in Fig. 9.

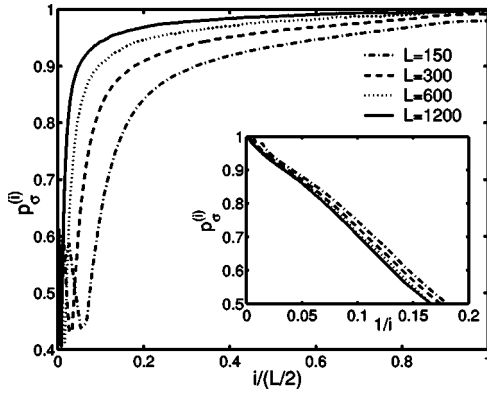


FIG. 9. The layer patch branching rate $p_\sigma^{(i)}$ plotted against $i/(L/2)$ for $\epsilon=0$ and a variety of system sizes. The inset shows the same data plotted against $1/i$ for layers near the center of the lattice.

For an extensive region in the center of the lattice we find that $p_\sigma^{(i)}$ approaches 1 as the system size increases, supporting the conjecture that all sites in a given w patch topple in the same avalanche. Plotting $p_\sigma^{(i)}$ against $1/i$ more clearly demonstrates the approach to 1 for layers sufficiently far from the boundary, as shown in the inset of Fig. 9.

We further need to establish that the size of w patches grows with L in order to claim criticality. A simple measure of this is to determine the average size of the largest patch, which we find does grow proportionally with L . It is also useful to develop a layer quantity which can be coupled with $p_\sigma^{(i)}$. For each layer we calculate the average largest unbroken sequence of sites with the same w value, divided by the number of sites in the layer. The resulting indicator— $\bar{d}^{(i)}$, say—approaches 1 if all sites in the layer are always part of a single patch and tends to $1/[4(L-2i+1)]$ if the w values in the layer are randomly distributed. Concentrating on $\epsilon=0$ and a range of L values reveals that $\bar{d}^{(i)} \rightarrow 0$ in the outer few layers (for $0 < i \leq L/20$) but converges to a finite nonzero value for all other layers. Combining the results for $p_\sigma^{(i)}$ and $\bar{d}^{(i)}$ suggests that the two-variable model is critical. With the exception of the outermost layers the size of w patches grows with L and within patches the sites generally all topple together. This results in a very inhomogeneous system, with the largest events typically occurring near the center of the lattice. The distribution of patch sizes over a large number of avalanches essentially corresponds to the avalanche probability distribution $P_L(s; \epsilon)$ discussed in Sec. II.

From the description above one is led to question whether the two-variable model leads to periodic behavior near the center of the lattice. Such behavior would raise doubts over the criticality of the model and more importantly greatly limit its applicability to natural phenomena. Simulations suggest that the disorder caused by the outer layers prevents a simple periodically repeating sequence of avalanches. More specifically the spatial inhomogeneity caused by the open boundary conditions stops a periodic state developing; thus, one finds large patches break into smaller ones while distinct

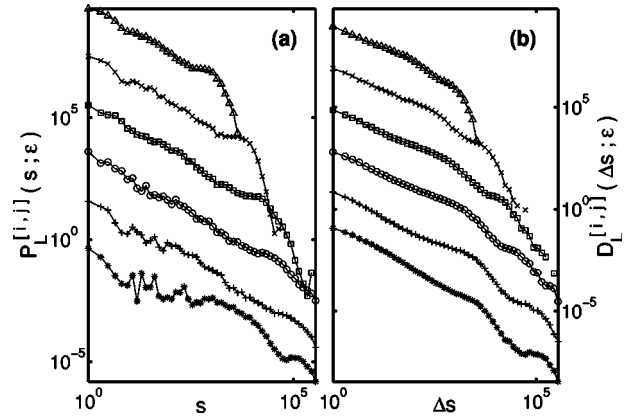


FIG. 10. The distributions (a) $P_L^{[i,j]}(s; \epsilon)$ and (b) $D_L^{[i,j]}(\Delta s; \epsilon)$ described in the text for $\epsilon=0$, $L=1200$, and a range of lattice coordinates (i, j) . From top to bottom the curves represent $i=j=100$ (shifted upwards by ten decades), $i=j=200$ (shifted upwards by eight decades), ..., $i=j=500$ (shifted upwards by two decades), and $i=j=600$.

patches may also merge into one.² To demonstrate this we have examined the event size distributions $P_L^{[i,j]}(s; \epsilon)$ which only count events that include the specific site (i, j) . In Fig. 10(a) we show the results for six sites spread across the lattice for the case $\epsilon=0$, $L=1200$.

In all cases we find approximate power-law behavior with no peaks characteristic of periodicity (note that because only events involving a specific site are included much less data are available leading to noisier plots). The maximum event size cutoff is larger for sites nearer the center of the lattice, as anticipated from the event size inhomogeneity described earlier. We have also recorded the difference in size (Δs) of successive events involving site (i, j) , collecting the results into another distribution function $D_L^{[i,j]}(\Delta s; \epsilon)$. If the size and location of events typically change slowly over time, we would expect $D_L^{[i,j]}(\Delta s; \epsilon)$ to be localized around $\Delta s \approx 0$; however, as shown in Fig. 10(b) the distribution is again approximately power law over several decades. These results are all consistent with the idea that the model is genuinely critical and a reasonable prototype for understanding the elements underlying physical phenomena such as earthquakes. One does sometimes find sequences of large avalanches for successive events including a specific site, which is unphysical. However, one must accept that simplifications in the model, such as having the same driving rates and ϵ values for every site, are also unphysical. The two-variable model is robust to variations in ϵ and the system driving rate which provides encouragement that further, more realistic, modifications will still result in a critical system with appropriate exponents.

Finally in this section it is interesting to note that one can repeat the analysis discussed above for more general definitions of a two-variable model; for example, one could replace the toppling rule for u in Eq. (2.1) by

²In contrast, when periodic boundary conditions are employed the two-variable model enters a stable periodic state attributable to synchronization.

$$u_{\text{neigh}} \rightarrow u_{\text{neigh}} + \alpha u_{ij}, \quad (4.3)$$

where $0 < \alpha \leq 0.25$. Preliminary studies for $\alpha < 0.25$ suggest that the system still organizes in such a way that large patches of constant w values are formed near the center of the lattice (so that $\bar{d}^{(\text{layer } i)} > 0$ throughout the interior of the system as above). However, one finds $p_{\sigma}^{(\text{layer } i)}$ does not approach 1 for any layer i so that the system is not critical even in the innermost region. Thus it seems likely that the conservation of the u variable in the toppling rule is essential for criticality in the two variable model.

V. DISCUSSION AND CONCLUSIONS

In summary, we have studied a generalized two-variable model as a prototype for self-organized critical behavior in nonconservative systems. Unlike the OFC model the two-variable model does appear to be genuinely critical in the nonconservative regime, at least near the center of the lattice, and further displays the power-law exponents observed in real dissipative processes such as earthquakes without any tuning of the model parameters (in this case ϵ). Furthermore, the model predicts universal behavior for all dissipative choices of ϵ if sufficiently large systems are considered.

In our presentation we have avoided making a strong connection between the two variables in the model and real physical systems. This is partly because such justification is already available in the literature, an excellent and detailed argument supporting the introduction of the $\epsilon=0$ version of the model to describe landslide events driven by homoge-

neous tilting being provided in [15]. More importantly we believe it is the insensitivity of the results to model details rather than a direct connection with one physical problem that is the strength of the model. The goal of the subject is to understand which elements are essential for explaining the ubiquity of apparently SOC behavior in a range of phenomena with different physical driving mechanisms and characteristics. We fully accept that the two-variable model may need to be extended or adapted in different ways to provide any realistic description of a specific phenomenon. However, the robustness of our results to variations in a range of parameters (driving rates, dissipation level, etc.) suggests that one may realistically obtain similar results in more complicated models. Thus the two-variable model contains all of the elements necessary to obtain SOC in dissipative systems and should be viewed as the simplest “toy” model for understanding this behavior. On the basis of the study in this paper two key elements have been identified. First, the failure of the random-neighbor version of the model indicates that spatial correlation is essential. Second, at least two variables are required to describe a dissipative system, with our analysis suggesting that if variables are distributed to neighboring sites in the toppling process, the redistribution needs to be conservative for criticality.

ACKNOWLEDGMENT

This research was supported in part by The Royal Society, U.K.

-
- [1] P. Bak, C. Tang, and K. Wiesenfeld, Phys. Rev. Lett. **59**, 381 (1987); Phys. Rev. A **38**, 364 (1988).
 - [2] For reviews see H. J. Jensen, *Self-Organized Criticality* (Cambridge University Press, Cambridge, England, 1998); D. L. Turcotte, Rep. Prog. Phys. **62**, 1377 (1999).
 - [3] T. Hwa and M. Kardar, Phys. Rev. Lett. **62**, 1813 (1989); S. S. Manna, L. B. Kiss, and J. Kertész, J. Stat. Phys. **61**, 923 (1990).
 - [4] Z. Olami, H. J. S. Feder, and K. Christensen, Phys. Rev. Lett. **68**, 1244 (1992); K. Christensen and Z. Olami, Phys. Rev. A **46**, 1829 (1992).
 - [5] H.-M. Bröker and P. Grassberger, Phys. Rev. E **56**, 3944 (1997).
 - [6] M.-L. Chabanol and V. Hakim, Phys. Rev. E **56**, R2343 (1997).
 - [7] P. Grassberger, Phys. Rev. E **49**, 2436 (1994).
 - [8] O. Kinouchi and C. P. C. Prado, Phys. Rev. E **59**, 4964 (1999).
 - [9] J. X. de Carvalho and C. P. C. Prado, Phys. Rev. Lett. **84**, 4006 (2000); **87**, 039802 (2001).
 - [10] K. Christensen, D. Hamon, H. J. Jensen, and S. Lise, Phys. Rev. Lett. **87**, 039801 (2001).
 - [11] G. Miller and C. J. Boulter, Phys. Rev. E **66**, 016123 (2002).
 - [12] C. J. Boulter and G. Miller, Phys. Rev. E **68**, 056108 (2003).
 - [13] S. Lise and M. Paczuski, Phys. Rev. E **63**, 036111 (2001).
 - [14] S. Hergarten and H. J. Neugebauer, Phys. Rev. E **61**, 2382 (2000).
 - [15] S. Hergarten, *Self-Organized Criticality in Earth Systems* (Springer-Verlag, Berlin, 2002).
 - [16] L. P. Kadanoff, S. R. Nagel, L. Wu, and S. Zhou, Phys. Rev. A **39**, 6524 (1989).
 - [17] S. Lise and H. J. Jensen, Phys. Rev. Lett. **76**, 2326 (1996).